Polymerization Effects on the Decomposition of a Pyrazolo-Triazine at high Temperatures and Pressures

Yaojiang Li, Junying Wu,* Lijun Yang, Deshen Geng, Manzoor Sultan, and Lang Chen[a]

4-amino-3-aminopyrazole-8-trinitropyrazolo-[5, 1-c] [1, 2, 4] triazine (PTX, $C_5H_2N_8O_6$) has good detonation performance, thermal stability and low mechanical sensitivity, which endow it with good development prospects in insensitive ammunition applications. To study the effects of polymerization on the decomposition of PTX, the reaction processes of PTX at different conditions were simulated by quantum chemistry and molecular dynamics methods. In this paper, the effects of polymerization on the decomposition of PTX were studied in terms of species information, reaction path of PTX, bond formation and bond cleavage, evolution of small molecules and clusters, and kinetic parameters at different stages. The results show that under the high-temperature and high-pressure conditions, the initial reaction path of unimolecular PTX in the thermal decomposition is mainly the cleavage of C–NO_2 bonds. At the same time, there are many polymerization reactions in thermal decomposition process, which may greatly affect the reaction rate and path. The higher the degree of polymerization, the larger equilibrium value of potential energy, the less energy release of thermal decomposition. Compared with the activation energy of other explosives, the activation energy of PTX is higher than that of β-HMX and lower than that of TNT.

1. Introduction

Fused-ring heterocycle 4-amino-3,7,8-trinitropyrazolo-[5,1-c] [1,2,4]triazine (PTX) is a new high-performing and low-sensitivity explosive. It was first synthesized by Dalinger in 2010.[1] PTX has molecular structure characteristics similar to 2,4,6-triamino-1,3,5-trinitro-benzene (TATB), 2,2-dinitroethene-1,1-diamine (FOX-7), 3,3′-diamino-4,4′-azoxyfurazan (DAAF), and 2,6-diamino-3,5-dinitropyrazine-1-oxide (LLM-105), such as flat molecular geometry, NH…O-type hydrogen bonds and π-π interactions,[2–5] and it also has properties similar to 1,3,5,7-tetranitro-1,3,5,7-tetraazacyclooctane (HMX) and 2,4,6,8,10,12-hexanitro-2,4,6,8,10,12-heaazaisowurtzitane (CL-20), such as high density and good oxygen balance.[6–7] Compared to HMX, PTX has similar explosive performance, low sensitivity and good thermal stability. In the initial synthesis stage, the overall yield of PTX was just 10%; thus, it was difficult to realize its large-scale production. In 2015, Schulze et al. optimized the synthetic route of PTX to achieve a 30% overall yield in a three-step synthesis.[8] Due to its excellent explosive properties, thermal safety performance and low sensitivity, with the further development of synthesis technology, PTX is expected to become a very promising explosive.

To study the effects of polymerization on the decomposition of PTX, researching the chemical reaction process from the microscopic level of atoms and molecules is necessary. Reactive molecular dynamics simulations can be performed on systems of up to millions of atoms.[9–10] Microscopic reaction information such as the initial reaction pathway of the high-temperature thermal decomposition of an energetic material, the reaction process of an intermediate product, and the evolution of the final product is obtained at the atomic or molecular scale. The chemical reaction process and mechanism are analyzed at the microscopic level by simulating the cleavage and formation of chemical bonds between atoms, which is of great significance for revealing the effects of polymerization on the decomposition of PTX.

The reactive force field plays a crucial role in molecular dynamics simulation, and its accuracy directly affects the precision of the simulation calculation results. In 2001, Van Duin et al.[11] established a reactive force field (ReaxFF) that describes the chemical reaction of materials. The calculation cost of the force field is low, and millions of atomic calculations can be performed. Reaction molecular dynamics simulation based on the ReaxFF was widely used in the calculation of single-compound explosives such as 1,3,5-trinitro-1,3,5-triazacyclohexane (RDX), nitromethane (NM), HMX, and CL-20 and the calculation of eutectic explosives.[12–23]

However, the ReaxFF cannot precisely describe the weak interactions of the crystal structure and density of a material and can thus produce large errors in the calculation. Liu et al.[24] used the low-gradient correction method to improve the ReaxFF by adding the London dispersive force term and modifying the long-range intermolecular interaction force, and they named the improvement ReaxFF/lg. Yang et al.[25] used the ReaxFF/lg to calculate the activation energy of CL-20 and CL-20/DNB (DNB, 1,3-dinitrobenzene) co-crystal, and the calculated activation energy of thermal decomposition was in good

[a] Y. Li, Prof. J. Wu, L. Yang, D. Geng, M. Sultan, L. Chen
State Key Laboratory of Explosion Science and Technology
Beijing Institute of Technology
No.5 Yard, Zhong Guan Cun South Street, Haidian District, Beijing (China)
E-mail: wjy1312@bit.edu.cn

Supporting information for this article is available on the WWW under https://doi.org/10.1002/open.202000006

agreement with the experimental value. In the simulation of trinitrotoluene (TNT) thermal decomposition with the ReaxFF and ReaxFF/lg, it was found that ReaxFF/lg provided more accurate calculations of the equilibrium density of TNT than ReaxFF.[26] Wang et al.[27] used the ReaxFF/lg to research the thermal decomposition process of CL-20 at different densities and analyzed the effect of density on the reaction mechanism; it was concluded that the initial reaction pathways of CL-20 at different densities were the same and that the initial density has little effect on the activation energy of the CL-20 reaction. The above studies indicate that the ReaxFF/lg has been widely used in the calculation of explosive reactions.

In this paper, based on the ReaxFF/lg, the thermal decomposition of PTX at different temperatures and densities (2000, 2500, 3000, 3500, 4000, and 4200 K; 1.979, 2.400, 2.668, and 2.823 $g \cdot cm^{-3}$) was numerically calculated. The effects of polymerization on potential energy, small molecules and clusters, bond formation and cleavage, and initial reaction path were analyzed. Kinetic parameters at different stages were obtained. These findings facilitate the study of the effects of polymerization on the decomposition of PTX and provide theoretical guidance for the safety analysis of PTX.

Experimental Section

Supercell

A 3×3×2 PTX supercell structure was built on the basis of the unit cell by using the Material Studio (MS). The PTX unit cell structure was derived from an X-ray diffraction crystal database, as shown in Figure 1.[8] The PTX supercell structure contained 72 molecules (1512 atoms). In this paper, large-scale atomic/molecular parallel simulation software (LAMMPS) was used to calculate the thermal decomposition of the PTX supercell at different temperatures and pressures by using the ReaxFF/lg reactive force field.

Force Field Applicability

The ReaxFF/lg is applicable to PTX explosive, which is a prerequisite for the accurate calculation of PTX reaction kinetics. To verify the applicability of the force field, the supercell was first geometrically optimized to obtain the initial configuration with the lowest potential energy. Then, the temperature relaxation of the PTX supercell was performed under the NVT ensemble, which used the Berendsen thermal bath method to raise the molecular temperature from 0 K to 300 K; the relaxation time was 5 ps. After that, the NPT ensemble was used to perform pressure relaxation at 0 GPa with 5 ps. Finally, the PTX equilibrium crystal structure at room temperature was obtained, as shown in Figure 2. Table 1 shows that the calculated unit cell parameters and density are in good agreement with the experimental values. To further verify the applicability of the force field, the structure of PTX was optimized by Gaussian09 quantum software with the DFT method at the B3LYP/6-311 g (d, p) level. Bond length information of the unit cell was obtained, as shown in Table S1 (Supporting information). The bond lengths and bond angles calculated with ReaxFF/lg were basically consistent with the values calculated via quantum chemistry method and the molecular structure was not distorted, which indicates that the ReaxFF/lg reactive force field suitably described the single molecular structure of PTX and that the precision was within an acceptable range.

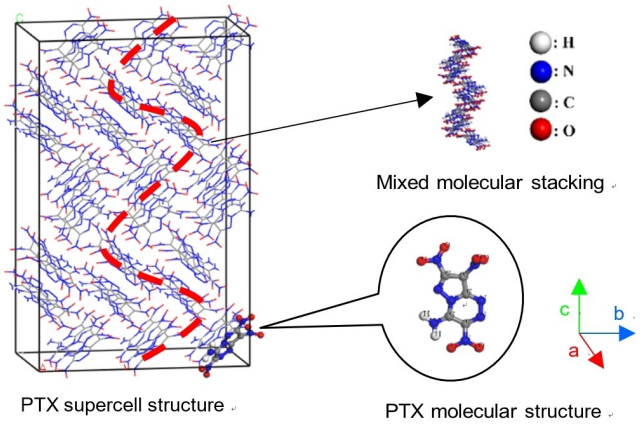

Figure 1. Schematic diagram of PTX molecular structure.

Calculation Parameter Settings

After obtaining the equilibrium crystal structure, the NPT ensemble was used to apply pressures of 1 atm, 10, 25 and 36 GPa (36 GPa was the detonation pressure of PTX) to the equilibrium structure. Then, the temperature and pressure were controlled by the Nose-Hoover hot bath and a pressure bath, and we obtain supercells with densities of 1.979, 2.400, 2.668 and 2.823 $g \cdot cm^{-3}$. After obtaining supercells with different densities, the NVE ensemble and

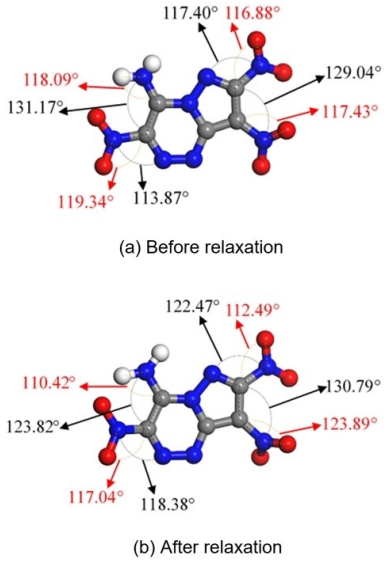

Figure 2. PTX molecular configuration before and after relaxation.

Table 1. The cellular parameters of PTX crystals at room temperature.

PTX	*a*/Å	*b*/Å	*c*/Å	ρ/g·cm^{-3}
Reference	5.26	8.59	20.39	1.95
ReaxFF/lg	5.23	8.53	20.25	1.99
Error/(%)	0.57	0.70	0.69	2.05
Parameter	α /°	β /°	γ /°	*V*/Å^3
Reference	90.0	90.0	90.0	921.99
ReaxFF/lg	90.0	90.0	90.0	902.74
Error/(%)	0	0	0	2.06

the Berendsen thermal bath method were used to rapidly heat each supercell to high temperatures (2000, 2500, 3000, 3500, 4000 and 4200 K). In this way, a supercell in a high-temperature and high-pressure state was obtained. In this state, atomic trajectories, species information, and bond-order information were recorded every 50 fs. To study the rapid chemical reaction of PTX, the time step was set to 0.1 fs. Every atom pair used a bond-order cutoff radius as a criterion for the formation of the product. When the bond-order radius of any atom pair is greater than 0.3, the old chemical bond is considered to be broken, and a new molecule is produced. Finally, the thermal decomposition processes under 24 conditions of high temperature and high pressure were calculated.

2. Results and Discussion

2.1. Potential Energy

The trend of potential energy at different densities is consistent. Figure 3 shows the evolution of the PTX potential energy of different densities at 3000 K. First, the potential energy of the system rises rapidly to a peak in a very short time. After that, the potential energy decreases rapidly. In a later stage of the reaction, the potential energy decreases slowly and finally reaches to stable state, and the supercell system reaches equilibrium. The equilibrium value of the potential energy increases with increasing density. At densities of 1.979, 2.400, 2.668 and 2.823 $g \cdot cm^{-3}$, the endothermic stage last for 0.65, 1.1, 0.75, and 0.20 ps, respectively, which indicate that the time required for the endothermic reaction stage of the PTX supercell first increases and then decreases with increasing density. This phenomenon can possible be explained by two different mechanisms. The first was proposed in Rom et al.[13] They believed that, at low density, unimolecular reactions primarily occur, and the surrounding molecules absorb energy from excited molecules, reducing the energy of the excited molecules. As the density increases, the interaction between the surrounding molecules and the excited molecules increases, thereby increasing the time of the endothermic stage. Bimolecular reactions occur when the density exceeds a certain value. For bimolecular reactions, increasing the density reduces the space between the molecules, which facilitates the chemical reaction, thereby increasing the reaction rate and shortening the endothermic reaction stage. The other mechanism was proposed by Zhou et al.[14] In their view, the initial decomposition pathway through bond breaking dominates at low pressure. As the density increases, the distance between the atoms decreases, the bond energy increases, and bond breaking becomes more difficult, thereby increasing the length of the endothermic stage. At high density, the molecules are severely deformed, the molecular spacing is reduced, and adjacent nonbonding atoms in the molecule or within the molecule more readily come into contact with each other, resulting in the formation of macromolecular clusters and rapid exotherm, which shorten the endothermic stage.

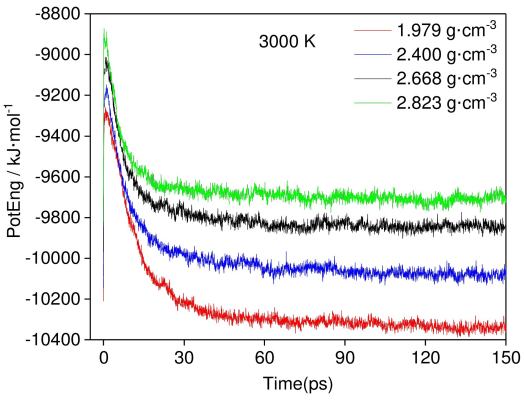

Figure 3. Evolution of potential energy for PTX of different densities at 3000 K.

2.2. Reaction Path of PTX

Research on the decomposition path of PTX under different conditions is beneficial to our understanding of the PTX reaction mechanism. Here, the unimolecular reactions and polymerization reactions were analyzed. To analyze the effects of polymerization on the reaction path of PTX, the bond-order files at the first 10 ps (PTX molecule has completely reacted) were analyzed. For a low degree of polymerization (1.979, 2.400 $g \cdot cm^{-3}$), there are many unimolecular reactions and polymerization reactions; for a high degree of polymerization (2.668, 2.823 $g \cdot cm^{-3}$), almost only polymerization reactions occur.

Table 2 shows the unimolecular reactions of different densities at 3000 K. At the 4 different densities, the reaction paths and frequencies are different. The increasing density reduces the gap between the molecules, which leads to a decrease in the number of unimolecular reactions. At 3000 K, there are 5 unimolecular reaction paths. There are more unimolecular reactions at 1.979 $g \cdot cm^{-3}$ than at the other three densities; thus, the frequency of 1.979 $g \cdot cm^{-3}$ is analyzed. At 1.979 $g \cdot cm^{-3}$, the reaction with the highest reaction frequency is equation (1), and the frequency is 7; the reaction with the second highest reaction frequency is equation (4), and the frequency is 5; and the reactions with the third highest reaction frequency are equations (2), (3) and (5), and the frequencies are 1. Among these 5 unimolecular reaction pathways, the reaction

Table 2. Unimolecular reactions of PTX of different densities at 3000 K.

T/K	ρ /g ·cm^{-3}	Frequency	Reaction time/ps	Primary reaction
3000	1.979	7	0 ~ 0.55	$C_5H_2N_8O_6 \rightarrow NO_2 + C_5H_2N_7O_4$
		5	1.25 ~ 6.20	$C_5H_2N_8O_6 \rightarrow NO + C_5H_2N_7O_5$
		1	0.15 ~ 0.15	$C_5H_2N_8O_6 \rightarrow H + C_5HN_8O_6$
		1	0.55 ~ 0.55	$C_5H_2N_8O_6 \rightarrow N_2 + C_5HN_6O_6$
		1	0.20 ~ 0.20	$C_5H_2N_8O_6 \rightarrow H_2N + C_5N_7O_6$
	2.400	2	0.10 ~ 1.25	$C_5H_2N_8O_6 \rightarrow NO + C_5H_2N_7O_5$
		1	0.05 ~ 0.05	$C_5H_2N_8O_6 \rightarrow NO_2 + C_5H_2N_7O_4$
		1	0.65 ~ 0.65	$C_5H_2N_8O_6 \rightarrow N_2 + C_5HN_6O_6$
	2.668	1	0 ~ 0	$C_5H_2N_8O_6 \rightarrow NO_2 + C_5H_2N_7O_4$
		1	0.10 ~ 0.10	$C_5H_2N_8O_6 \rightarrow H_2N + C_5N_7O_6$
	2.823	1	0.85 ~ 0.85	$C_5H_2N_8O_6 \rightarrow NO_2 + C_5H_2N_7O_4$

of PTX decomposition to NO_2 is the main initial unimolecular reaction.

$$C_5H_2N_8O_6 \rightarrow NO_2 + C_5H_2N_7O_4 \quad (1)$$

$$C_5H_2N_8O_6 \rightarrow N_2 + C_5H_2N_6O_6 \quad (2)$$

$$C_5H_2N_8O_6 \rightarrow H_2N + C_5N_7O_6 \quad (3)$$

$$C_5H_2N_8O_6 \rightarrow NO + C_5H_2N_7O_5 \quad (4)$$

$$C_5H_2N_8O_6 \rightarrow H + C_5HN_8O_6 \quad (5)$$

Through the analysis of atomic snapshots, we can visually see the specific process of PTX decomposition to NO_2. The primary unimolecular reaction are divided into 3 types of path. The first path is the cleavage of the C–NO_2 bond on the five-membered ring to produce NO_2. The second path is the cleavage of the C–NO_2 bond on the six-membered ring to produce NO_2. The third path is the cleavage of the other C–NO_2 bond on the five-membered ring to produce NO_2. In this paper, the Gaussian09 program with a B3LYP-6-311 g (d, p) basis set was used to calculate the energy barriers of path 1, 2 and 3. The calculation results are shown in Figure 4. Among 3 different reaction paths, the path 1 has the lowest energy barrier, which indicates that the number of initial unimolecular reactions through the path 1 may be more than those of the path 2 and 3.

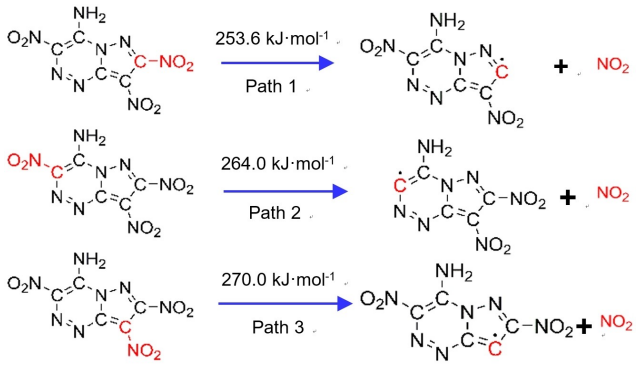

Figure 4. Energy barriers of path 1, 2 and 3.

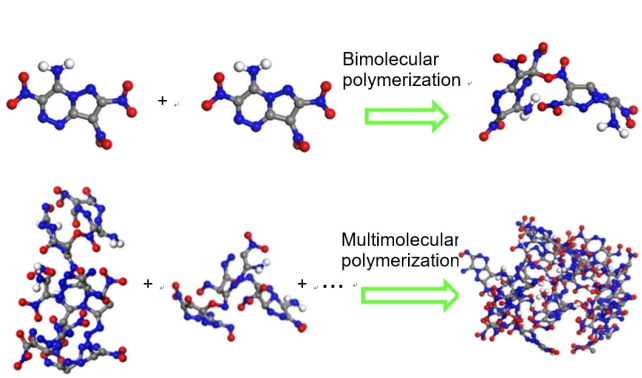

Figure 5. Polymerization of PTX.

Table S2 (Supporting information) shows the main polymerization reactions of the first 0.3 ps at different densities. When PTX molecules are polymerized, they form clusters through the formation of C–O bonds. At 1.979, 2.400, 2.668 and 2.823 g·cm^{-3}, the maximum molecular masses of the first 0.3 ps are 1080, 3705, 4224 and 17488, respectively, which indicates that the higher the density, the higher degree of polymerization. In addition, at the different 4 densities, PTX molecules first form small clusters, and then small clusters form large clusters, as shown in Figure 5.

2.3. Species

Figure 6 shows the evolution of species in the PTX supercell at different densities. The higher the density, the greater the number of PTX molecules that undergo polymerization, and the higher the degree of polymerization, the greater the molecular weight of the polymer. As seen from Figure 6, the number of species decreases as the degree of polymerization increases. As the reaction progresses, the number of species decreases and finally reaches a certain equilibrium value. At 1.979 g·cm^{-3}, the polymerization degree of the system is relatively low, the number of species reaches a maximum of 94 at 6.15 ps, and the final equilibrium value is approximately 60; at 2.400 g·cm^{-3}, the polymerization degree of the system increases, the number of species reaches a maximum of 70 at 12.8 ps, and the final equilibrium value is approximately 48; at 2.668 g·cm^{-3}, the polymerization degree of the system further increases, the number of species reaches a maximum of 54 at 30.8 ps, and the final equilibrium value is approximately 42; and at 2.823 g·cm^{-3}, the polymerization degree of the system reaches the maximum, the number of species reaches a maximum of 45 at 57.3 ps, and the final equilibrium value is approximately 38. With the increase in the polymerization degree of the system, the time at which the PTX supercell reaches the maximum number of species increases, and the final equilibrium number of species decreases. At a lower degree of polymerization, there are more unimolecular reactions in the PTX supercell and more small clusters. PTX unimolecular reactions rapidly generate a large number of small molecules, and so the number of species

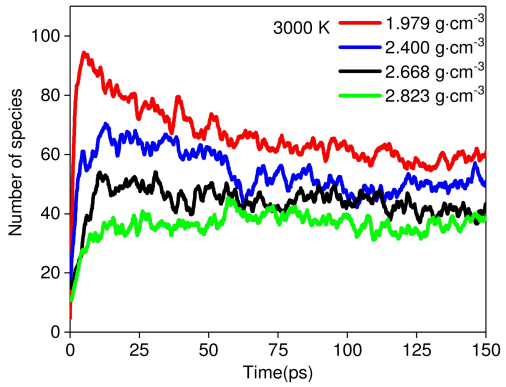

Figure 6. Evolution of total species for PTX supercell at 3000 K.

increases rapidly. At a higher degree of polymerization, more PTX polymerizes to form clusters, and some of the clusters further combine to form large clusters, which increases the time at which the PTX supercell reaches the maximum number of species and decreases the final equilibrium number of species. The above results indicate that the occurrence of polymerization affects the number of species in the decomposition process of PTX.

2.4. Bond Formation and Cleavage of PTX

Before the analysis of bond formation and bond cleavage, this paper defines the ratio X of the formation or cleavage of any bond type as:

$$X = \frac{N_F - N_C}{N} \tag{6}$$

N_F is bond formation, N_C is bond cleavage, and N is the max number of certain bond formation or certain bond cleavage.

When the degree of polymerization of the system is low (1.979 and 2.400 $g \cdot cm^{-3}$), there are more unimolecular reactions. The stable value of the C–O bond is approximately 64%, 68%, and a large number of C–O bonds are formed due to the generation of a large amount of the final product CO_2. This result can be demonstrated through small molecule analysis. When the degree of polymerization of the system is high (2.668 and 2.823 $g \cdot cm^{-3}$), there are more polymerization reactions. The stable value of the C–O bond is about 69%, 72%, and the PTX molecules are mostly polymerized into clusters in the form of C–O bonds; thus, C–O bond formation increases. It is shown in Figure 7 that the rate of bond formation and the stable value of the C–O bond at a high degree of polymerization are higher than those at a low degree of polymerization. Therefore, polymerization has an effect on the bonding rate and the number of C–O bonds in the process of PTX decomposition.

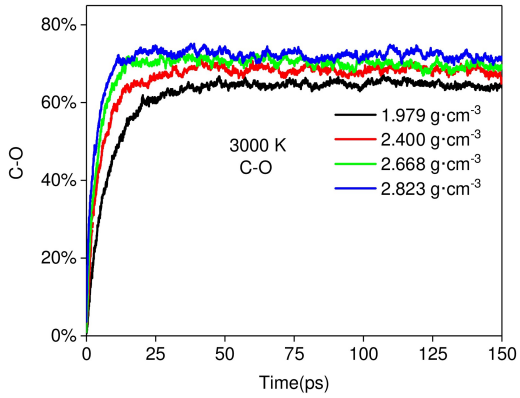

Figure 7. Relative bond change of C–O at 3000 K.

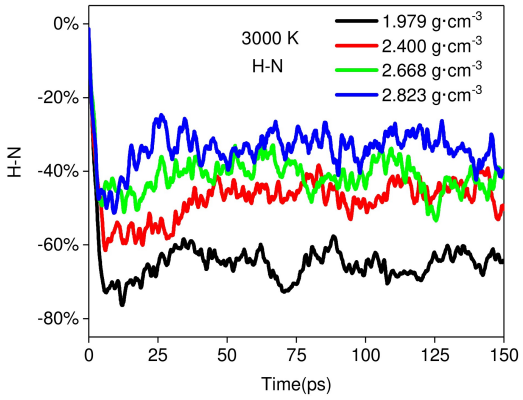

Figure 8. Relative bond change of H–N at 3000 K.

The polymerization reaction also affects the cleavage of H–N bonds. It can be seen from Figure 8 that, for a low degree of polymerization (1.979 and 2.400 $g \cdot cm^{-3}$), the number of H–N bonds that are cleaved is large, and the stable value of H–N bonds is approximately 67%, 46%. The H–N bond breaks, and H atoms combine with O and C atoms to form new small molecules. For a high degree of polymerization (2.668 and 2.823 $g \cdot cm^{-3}$), the number of H–N bonds that are cleaved is small, and the stable value of the H–N bond is approximately 40%, 31%. More NH_2 groups will participate in the formation of clusters; thus, it is not easy for them to break and combine with other atoms.

2.5. Main Thermal Decomposition Products

2.5.1. Small Molecule Products

A molecule having a relative molecular mass lower than the relative molecular mass of the PTX molecule is defined as a small molecule. In this paper, the main small molecule products are NO_2, NO, HNO, HNO_2, CO_2, H_2O, N_2 and H_2. Among these small molecules, CO_2, H_2O, H_2, and N_2 are final products. The number of small molecules is divided by the total number of PTX molecules to obtain the number of small molecules produced by each PTX molecule.

Figure 9 shows the evolution of NO_2, NO, HNO and HNO_2 at 3000 K. At 1.979 $g \cdot cm^{-3}$, the number of small molecules follows the order $NO_2 > HNO > NO > HNO_2$; at 2.400 and 2.668 $g \cdot cm^{-3}$, the number of small molecules follows the order $NO_2 > NO > HNO > HNO_2$; and at 2.823 $g \cdot cm^{-3}$, the number of small molecules follows the order $NO_2 > HNO_2 > NO > HNO$. The results indicate that there are significant differences among the reaction paths of PTX at different degrees of polymerization, which also shows that polymerization has an effect on the reaction path of PTX.

The number of small molecules decreases as the degree of polymerization increases, which is consistent with the above results. The higher the density of PTX, the fewer unimolecular reactions and small molecules. As shown in Figure 9, at 4 different densities, NO_2 appears first, followed by NO. The rate of NO_2 formation is higher than that of NO, and the amount of NO_2 formed is higher than that of NO, which also indicates that the cleavage of the C–NO_2 bond to produce NO_2 is the primary initial reaction. When the number of small molecules reaches a

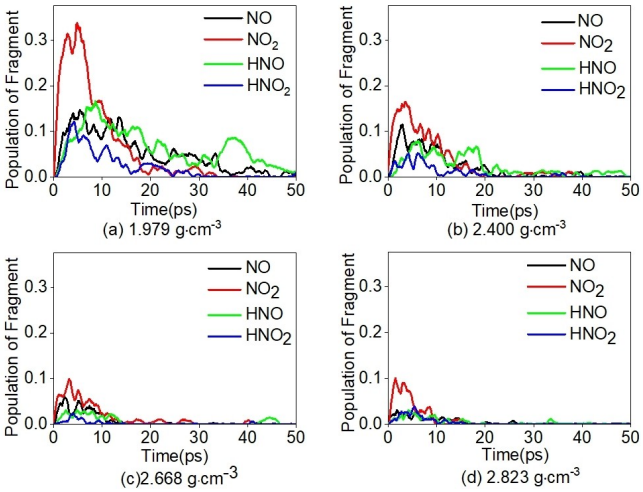

Figure 9. Evolution of NO, NO_2, HNO, and HNO_2 at 3000 K.

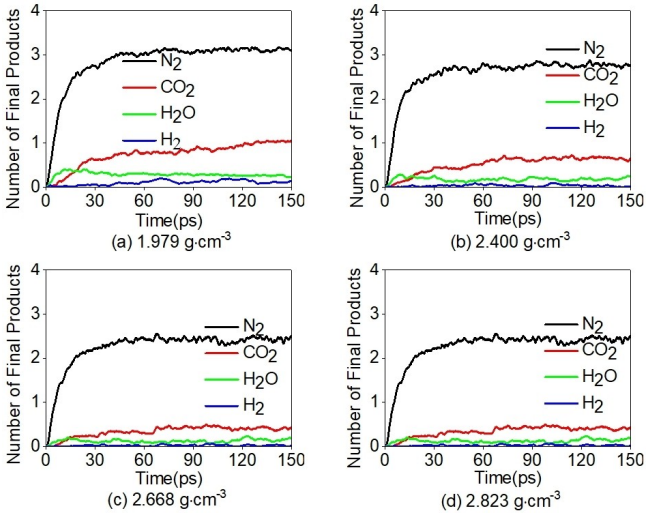

Figure 10. Evolution of CO_2, H_2O, N_2, H_2 at 3000 K.

maximum, this number decreases sharply. Small molecules transform toward the final product.

For a low degree of polymerization, there are many small molecule reactions. NO forms N_2 by combining with HN_2O and HN_2, NO_2 forms N_2 by combining with HN_2 and HN_2O.

$$NO + HN_2O \rightarrow N_2 + HNO_2 \quad (7)$$

$$NO + HN_2 \rightarrow N_2 + HNO \quad (8)$$

$$NO_2 + HN_2 \rightarrow N_2 + HNO_2 \quad (9)$$

$$NO_2 + HN_2O \rightarrow N_2 + HNO_3 \quad (10)$$

For a high degree of polymerization, the conversion of NO and NO_2 to the final product N_2 is often related to clusters.

$$\begin{aligned} &NO + HN_3O + H_2N_2O + CO_2 + C_{11}H_5N_{12}O_{15} + C_2O_2 + \\ &C_2HO_3 + C_{261}H_{73}N_{219}O_{284} + C_5O_8 + C_5H_2N_4O_5 + \\ &C_5H_4N_3O_7 \rightarrow 3\,N_2 + 2\,N_3 + HN_2 + HN_2O + H_2O + H_3N + \\ &H_3NO + C_{12}H_6N_{13}O_{13} + C_2O_3 + C_2HNO_3 + C_2HN_3O_3 + \\ &C_{262}H_{68}N_{199}O_{290} + C_4HNO_7 + C_8HN_9O_7 \end{aligned} \quad (11)$$

$$\begin{aligned} &2NO_2 + H_2N + C_{10}H_5N_{16}O_{13} + C_{110}H_{43}N_{174}O_{125} + \\ &C_{145}H_{55}N_{223}O_{165} + C_{30}H_{10}N_{47}O_{33} + C_{30}H_{12}N_{48}O_{34} + \\ &C_5HN_7O_6 + 2\,C_5H_2N_8O_6 \rightarrow 3\,N_2 + H_2O_2 + C_{10}H_4N_{16}O_{14} + \\ &C_{315}H_{118}N_{492}O_{359} + C_5H_2N_7O_4 + C_5H_3N_5O_6 + C_5H_3N_8O_7 \end{aligned} \quad (12)$$

Other small molecules such as HNO and HNO_2 are converted into H_2O and N_2 in some subsequent reactions.

Figure 10 shows the evolution of N_2, CO_2, H_2 and H_2O in the first 50 ps at 3000 K. The equilibrium amount of final products follows the order $N_2 > CO_2 > H_2O > H_2$; this relationship does not change with the degree of polymerization. The amount of final products decreases as the degree of polymerization increases.

For a high degree of polymerization, a large number of PTX molecules participate in the formation of clusters, and many atoms are limited in clusters, thus reducing the number of final products. The path to the final product varies according to the degree of polymerization. Here, N_2 is taken as an example for explanation.

For a low degree of polymerization, reaction path analysis indicates that N_2 is derived from two paths. Some N_2 is derived from the conversion of small molecules such as NO_2 and NO, but N_2 also comes from the ring of PTX. First, either the N–N bond on the five-membered ring or the C–N bond on the six-membered ring is broken; then, the broken ring produces small molecules such as $C_2N_2O_2$, $C_3N_4O_3$, and $C_2N_2O_3$:

$$C_5HN_6O_4 \rightarrow C_2N_2O_2 + C_3HN_4O_2 \quad (13)$$

$$C_5HN_6O_7 \rightarrow C_2N_2O_3 + C_3HN_4O_4 \quad (14)$$

$$C_5H_2N_5O_5 \rightarrow C_2H_2NO_2 + C_3N_4O_3 \quad (15)$$

With these reactions, small molecules such as $C_2N_2O_2$, $C_3N_4O_3$, and $C_2N_2O_3$ decompose and eventually produce N_2:

$$C_2N_2O_2 \rightarrow N_2 + C_2O_2 \quad (16)$$

$$C_2N_2O_3 \rightarrow N_2 + C_2O_3 \quad (17)$$

$$C_3N_4O_3 \rightarrow N_2 + C_3N_2O_3 \quad (18)$$

For a high degree of polymerization, N_2 is mainly derived from the formation or decomposition of clusters. PTX is first polymerized into clusters, accompanied by the production of small molecules during polymerization:

$$N_3 + H_2O + H_2N_2O_2 + H_3N + C_2O_3 + C_2NO_2 + C_3O_4 + C_3HN_3O_6 + C_{332}H_{83}N_{260}O_{363} \rightarrow 7\,N_2 + HO + HN_2 + 2HN_2O + CN_2O + C_2O_2 + C_2N_5O_3 + C_{328}H_{85}N_{238}O_{362} + C_9H_5N_6O_{10} \quad (19)$$

With this reaction, the cluster decomposes, and N_2 is produced in the process of cluster decomposition:

$$CO_2 + CN_4O + C_2O_3 + C_2N_3O_4 + C_{330}H_{93}N_{273}O_{362} + C_4H_3NO_5 \rightarrow 6\,N_2 + 3HO + HN_2 + HN_2O + H_2N_5O + CN_2O_2 + CHN_3O + C_2N_2O_3 + C_{328}H_{85}N_{249}O_{355} + C_4HN_3O_7 + C_4H_2NO_4 \quad (20)$$

In PTX, the mass fraction of N is 41.48%, and the mass fraction of O is 35.56%; the difference between the two mass fractions is only 5.92%. However, at 1.979, 2.400, 2.668 and 2.823 $g\cdot cm^{-3}$, the differences of N and O mass fractions in the final products of 150 ps are 39.70%, 48.3%, 56.37% and 64.86%, respectively, which are much higher than the initial differences. The results indicate that a considerable portion of the O atoms has not been released and that these O atoms are confined to clusters and cannot participate in the reaction.

2.5.2. Clusters

The clusters affect the chemical energy release rate of molecules and play a very important role in the chemical reaction.[28–29] Atomic polymers having a molecular mass greater than twice the molecular mass of PTX are defined as clusters.

The ratio of the maximum cluster molecular mass to the total supercell molecular mass is represented by γ, which can be used to measure the sizes of PTX clusters in different states. Figure 11 shows the evolution of γ at different densities. When the density is 1.979 $g\cdot cm^{-3}$, γ is relatively stable at 150 ps, and the equilibrium value is approximately 0.04, which indicates that the largest cluster during the PTX reaction contains approximately only 4% of PTX molecules. The degree of polymerization is low. At 2.400, 2.668 and 2.823 $g\cdot cm^{-3}$, the trends in the γ value within 150 ps are consistent; that is, it first increases, then decreases, and finally stabilizes. The equilibrium values of γ are 0.12, 0.34 and 0.42, respectively; that is, the largest cluster contains approximately 12%, 34%, and 42% of PTX molecules during the reaction process, respectively. The degrees of polymerization are relatively high. The higher the density, the more PTX molecules form the largest cluster.

At 1.979, 2.400, 2.668 and 2.823 $g\cdot cm^{-3}$, γ reaches maximum values at 4.25, 1.4, 0.9 and 0.8 ps, respectively, and the maximum values at each density are 0.07, 0.39, 0.81 and 0.93, respectively. This result indicates that the higher the density, the higher the degree of polymerization, and the faster the formation of clusters. Compared with the respective equilibrium values, the difference between the maximum value and the equilibrium value at 1.979 $g\cdot cm^{-3}$ is small, i.e., only 0.03. The differences between the maximum value and the equilibrium value at 2.400, 2.668 and 2.823 $g\cdot cm^{-3}$ are 0.27, 0.47, and 0.51, respectively, indicating that the higher the degree of polymerization, the greater the difference between the maximum value and the equilibrium value.

Figure 12 shows the evolution of γ for different densities at 3000 K. When the density is 1.979 or 2.400 $g\cdot cm^{-3}$, the number of clusters decreases. Figures 11 and 12 show that, at 2.400 $g\cdot cm^{-3}$, when the number of clusters over time decreases, the molecular mass of the largest cluster increases, which indicates that some small clusters combine to form larger clusters. At 2.668 or 2.823 $g\cdot cm^{-3}$, the number of clusters increases, while the largest cluster molecular weight decreases, which indicates that large clusters decompose into smaller clusters.

2.6. Reaction Kinetic Parameters

To study the effect of density on the reaction rate of PTX thermal decomposition, this paper used the reaction rate analysis method proposed by Rom.[13] This method divided the thermal decomposition reaction process into the endothermic reaction stage, exothermic reaction stage and final product evolution stage. By using Arrhenius's law to fit the activation energy of endothermic reaction and exothermic reaction stage. The degree of difficulty of the reaction can be analyzed. The relationship among the reaction rate constant, temperature, and activation energy is:

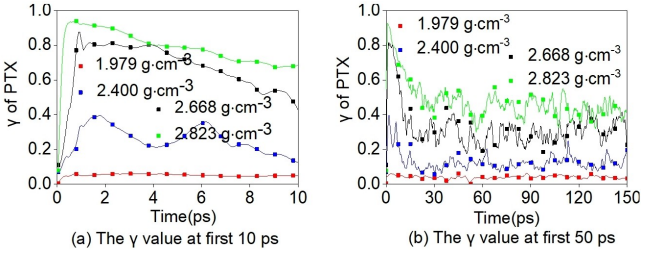

Figure 11. Evolution of γ with different densities at 3000 K.

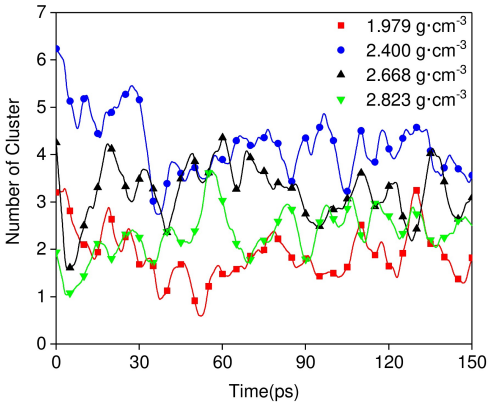

Figure 12. Evolution of Number of clusters with different densities at 3000 K.

$$\ln(k(T)) = \ln(A) - \frac{E}{RT} \quad (21)$$

T is the temperature, k is the reaction rate, A is the pre-exponential factor, E_a is the activation energy, and R is the ideal gas constant.

2.6.1. Endothermic Stage

The reaction rate in the endothermic stage was obtained by analyzing the evolution of the number of PTX molecules with time. The exponential function expression is:

$$N(t) = N_0 \cdot \exp[-k_1(t - t_0)] \quad (22)$$

N_0 is the initial number of PTX molecules, t_0 is the initial moment of the thermal decomposition of PTX, and k_1 is the reaction rate of the endothermic process.

In the endothermic reaction stage, the evolution of the number of PTX molecules was fitted using the equation to obtain the initial reaction rate k_1. Since the PTX reaction rate is extremely fast when T $\geq$ 4000 K, the data do not well describe the decay process of PTX and were not counted here.

Using the equation to fit the curve of the number of PTX molecules, the initial reaction rate k_1 at different temperatures and densities can be obtained, as shown in Table 3. At the same temperature, the value of k_1 increases with increasing density, and the higher the temperature, the greater the change in k_1. At the same density, k_1 increases with increasing temperature, and the higher the density, the greater the change in k_1. Therefore, increases in temperature and density could increase the value of k_1, but the reasons for these increases are not the same. An increase in temperature increases the rate of atomic velocity, resulting in an increase in k_1, while an increase in density causes an increase in the degree of polymerization, causing the number of PTX molecules to decrease rapidly, resulting in a rapid increase in k_1.

Table 3. Arrhenius parameters fitted to PTX exponential decay rates, k_1(ps^{-1}), over the Entire Simulation Period for various initial densities.

T/K	k_1/ps^{-1}			
	1.979 g·cm^{-3}	2.400 g·cm^{-3}	2.668 g·cm^{-3}	2.823 g·cm^{-3}
2000 K	0.16	0.19	1.13	3.24
2500 K	0.69	1.42	3.01	12.13
3000 K	1.60	2.86	5.81	19.52
3500 K	3.17	11.88	15.18	22.81

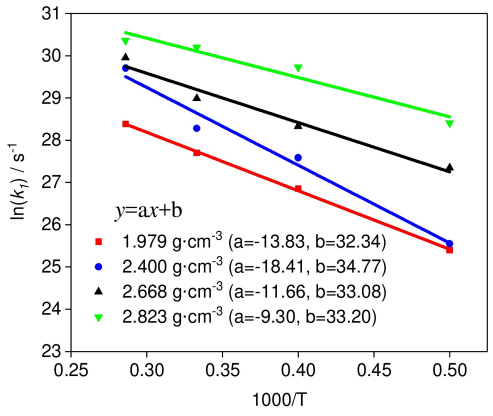

Figure 13. Logarithm of initial reaction rates vs inverse temperature from 2000–3500 K.

k_1 is fit by the Arrhenius formula, as shown in Figure 13. The figure shows that the slopes at different densities vary widely. The activation energy E_a of the endothermic stage at different densities is given in Table 4. The data in Table 4 show that the activation energy in the endothermic phase increases first and then decreases with increasing density, which is caused by the different paths of the initial reactions at different densities. When the density is 1.979, 2.400 g·cm^{-3}, there are many unimolecular reactions during thermal decomposition. In the reaction, the energy of the excited molecules can be absorbed by the surrounding molecules so that the energy of the excited molecules is reduced. As the density increases, the molecules around the excited molecules increase, causing the energy of the excited molecules to decrease faster. Therefore, the activation energy in the endothermic phase increases as the density increases. When the density is 2.668, 2.823 g·cm^{-3}, the initial reaction is mainly polymerization, and the increase in density decreases the spacing between molecules so that the polymerization reaction is more likely to occur. Therefore, the degree of polymerization has a great influence on the activation energy in the endothermic stage. The activation energy of PTX in the endothermic stage at atmospheric pressure was compared with the activation energy of other explosives (these explosives were calculated by the ReaxFF under zero- or atmospheric-pressure conditions) in the endothermic stage, as shown in Table 4.[9,30] The activation energy of PTX in the endothermic stage is higher than that of β-HMX and lower than that of TNT, which indicates that the energy required for the endothermic reaction of PTX is higher than that required for the endothermic reaction of β-HMX and lower than that required for the endothermic reaction of TNT.

2.6.2. Exothermic Stage

In the potential energy curve, the stage from the maximum value to the equilibrium value is called the exothermic stage. Using a first-order decay exponential formula to fit the potential

Table 4. Activation energy of PTX at different densities and for different explosives in the endothermic stage.

Explosives	ρ /g·cm^{-3}	E_a/kJ·mol^{-1}
PTX	1.979	115.0
	2.400	153.1
	2.668	96.91
	2.823	77.32
β-HMX[9]	1.770	104.9
TNT[30]	1.510	143.4

energy attenuation stage, the reaction rate expression for the PTX exothermic reaction stage can be obtained:

$$U(t) = U_\infty + \Delta U_{exo} \cdot \exp[-k_2(t - t_{max})] \quad (23)$$

$\Delta U_{exo} = U(t_{max}) - U_\infty$, U_∞ is the equilibrium value of the potential energy when time approaches infinity, $U(t_{max})$ is the maximum potential energy, and k_2 is the rate of the secondary reaction.

The potential energy curve of the exothermic stage was fitted to obtain the secondary reaction rate k_2. k_2 was fitted by the Arrhenius formula to obtain the activation energy for the exothermic stage at different densities, as shown in Table 5.

Table 5 shows that, at the same temperature, the value of k_2 increases as the density increases; at the same density, the value of k_2 increases with increasing temperature. The secondary reaction rate increases with increasing temperature and density. The Arrhenius formula was used to fit k_2, as shown in Figure 14. The slopes at each density are similar. Table 6 shows the activation energies at different densities in the exothermic stage. The degree of polymerization has little effect on the activation energy of the exothermic stage. Furthermore, the activation energy of PTX in the exothermic stage at atmospheric pressure is compared with the activation energy of other explosives (as calculated by the ReaxFF under zero- or atmospheric-pressure conditions) in the exothermic stage, as shown in Table 6.[9,30] The table shows that the activation energy of PTX in the exothermic stage is higher than that of β-HMX and lower than that of TNT, which indicates that the energy required for the exothermic reaction of PTX is higher than that required for the exothermic reaction of β-HMX and lower than that required for the exothermic reaction of TNT.

Tables 4 and 6 show that the activation energies of PTX in the endothermic and exothermic stages are higher than that of β-HMX and lower than that of TNT, which indicate that PTX is more difficult to react than β-HMX. Namely, the sensitivity of PTX is lower than that of β-HMX. This finding is consistent with the experimental results of Schulze et al.[8] The activation energies of PTX in the endothermic and exothermic stages are lower than that of TNT, which indicate that PTX is easier to react than TNT. Namely, the sensitivity of PTX is higher than that of TNT.

Table 5. Arrhenius parameters fitted to PE exponential decay rate, k_2(ps^{-1}), for various initial densities.

T/K	k_2/ps^{-1} 1.979 g·cm^{-3}	2.400 g·cm^{-3}	2.668 g·cm^{-3}	2.823 g·cm^{-3}
3000 K	0.07	0.10	0.12	0.14
3500 K	0.15	0.19	0.22	0.25
4000 K	0.25	0.31	0.39	0.45
4500 K	0.28	0.34	0.43	0.50

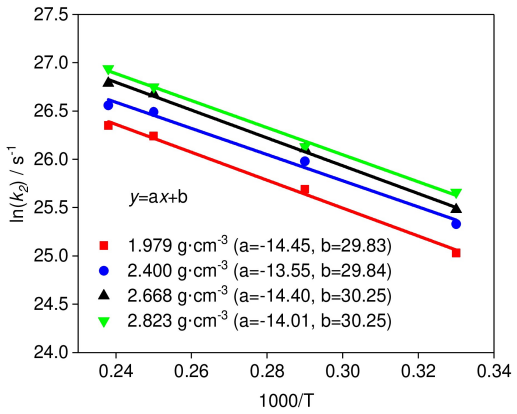

Figure 14. Logarithm of second reaction rates vs inverse temperature from 3000–4200 K.

Table 6. Activation energy of PTX at different densities and for different explosives in the exothermic stage.

Explosives	ρ /g·cm^{-3}	E_a/kJ·mol^{-1}
PTX	1.979	117.5
	2.400	109.4
	2.668	117.7
	2.823	113.3
β-HMX[9]	1.770	94.47
TNT[30]	1.510	157.6

2.6.3. Final Products Evolution

In the final product evolution stage, the variation in potential energy is very small, and the curve of the number of final product molecules of PTX thermal decomposition versus time was fitted with the following expression:

$$C(t) = C_\infty\{1 - \exp[-k_3(t - t_i)]\} \quad (24)$$

C_∞ is the equilibrium value of the product, t_i is the time at which the product appears, and k_3 is the formation rate of products.

The main final products of PTX thermal decomposition are N_2, CO_2, H_2O and H_2. As seen from Figure 10, the number of H_2O and H_2 molecules at 150 ps is extremely small, which is related to the fact that the PTX molecule contains little H. Compared to H_2O and H_2, N_2 and CO_2 are more abundant and stable at 150 ps; thus, only N_2 and CO_2 were fitted here. The final product of PTX thermal decomposition at different densities was fitted by the equation to obtain the final product formation rate k_3, as shown in Figure 15. With increasing degree of polymerization, the rate of N_2 formation increases, but the rate of CO_2 formation first increases and then decreases. The rates of N_2 and CO_2 formation are affected by the degree of polymerization.

3. Conclusion

The reaction processes of PTX at different temperatures and densities were numerically calculated by the molecular dynamics method and quantum chemistry calculation. The influence of polymerization on the PTX reaction was researched. In the decomposition reaction of PTX, the higher the degree of polymerization, the larger the potential energy equilibrium

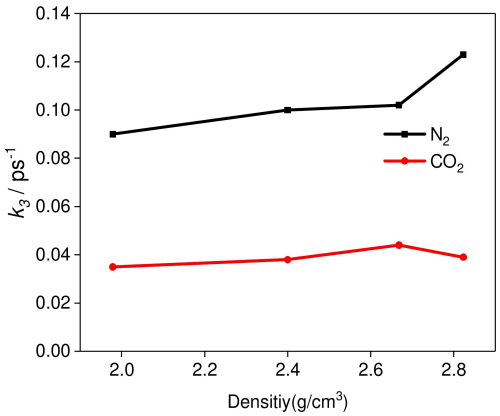

Figure 15. Reaction rate k_3 of CO_2, N_2 with different densities at 3000 K.

value, and the less energy released by PTX. The increase in the polymerization degree of the system reduced the number of species and affected the initial reaction path. For a low degree of polymerization, there are many unimolecular reactions and polymerization reactions; for a high degree of polymerization, many polymerization reactions occur. In the 5 unimolecular reaction paths, the initial reaction paths are dominated by cleavage of the C–NO_2 bond. For polymerization, the clusters are mainly formed by the combination of PTX molecules via C–O bond formation. The existence of polymerization also greatly affected bond formation and cleavage and the reaction path of small molecules. Polymerization also had an obvious effect on the activation energy of the endothermic stage of PTX. The activation energy of the endothermic stage increased first and then decreased with the increase in density, but the activation energy of the exothermic stage was hardly affected. The activation energy analysis indicates that the sensitivity of PTX is lower than β-HMX and higher than TNT.

Acknowledgements

This work was supported by the National Natural Science Foundation of China (grant numbers 11832006).

Conflict of Interest

The authors declare no conflict of interest.

Keywords: polymerization reactios · reaction kinetics · thermal decomposition · detonation performance · molecular dynamics

[1] I. L. Dalinger, I. A. Vatsadse, T. K. Shkineva, G. P. Popova, B. I. Ugrak, S. A Shevelev, *Russ. Chem. Bull.* **2010**, *59*, 1631–1638.
[2] A. J. Bellamy, S. J. Ward, P. Golding, *Propellants Explos. Pyrotech.* **2002**, *27*, 49–58.
[3] M. Anniyappan, M. B. Talawar, G. M. Gore, S. Venugopalan, B. R Gandhe, *J. Hazard. Mater.* **2006**, *137*, 812–819.
[4] E. C. Koch, *Propellants Explos. Pyrotech.* **2016**, *41*, 526–538.
[5] P. F. Pagoria, *Lawrence Livermore Lab. [Rep.] UCRL* **1998**.
[6] S. Bulusu, J. Autera, T Axenrod, *J. Labelled Compd. Radiopharm.* **1980**, *17*, 707–710.
[7] R. L. Simpson, P. A. Urtiew, D. L. Ornellas, G. L. Moody, K. J. Scribner, D. M Hoffman, *Propellants Explos. Pyrotech.* **1997**, *22*, 249–255.
[8] M. Schulze, B. Scott, D Chavez, *J. Mater. Chem. A* **2015**, *3*, 17963–17965.
[9] L. Zhang, S. V. Zybin, A. C. T. Van Duin, S. Dasgupta, W. A. Goddard, E. M Kober, *J. Phys. Chem. A* **2009**, *113*, 10619–10640.
[10] K. Chenoweth, S. Cheung, A. C. T. Van Duin, W. A. Goddard, E. M Kober, *J. Am. Chem. Soc.* **2005**, *127*, 7192–7202.
[11] A. C. T. Van Duin, S. Dasgupta, F. Lorant, W. A. Goddard, *J. Phys. Chem. A* **2001**, *105*, 9396–9409.
[12] A. Strachan, E. M. Kober, A. C. T. Van Duin, J. Oxgaard, W. A Goddard, *J. Chem. Phys.* **2005**, *122*, 54502.
[13] N. Rom, S. V. Zybin, A. C. T. Van Duin, W. A. Goddard, Y. Zeiri, G Katz, R Kosloff, *J. Phys. Chem. A* **2011**, *115*, 10181–10202.
[14] T. T. Zhou, F. L. Huang, *J. Phys. Chem. B* **2010**, *115*, 278–287.
[15] L. Zhang, L. Chen, C. Wang, J. Y Wu, *Acta Physicochim. URSS* **2013**, *29*, 1145–1153.
[16] L. Zhang, L. Chen, C. Wang, D. S. Geng, J. Y. Wu, J. Y. Lu, C Wang, *Explosion and Shock Waves* **2014**, *34*, 188–194.
[17] L. Zhang, S. V. Zybin, A. C. T. Van Duin, S. Dasgupta, W. A. Goddard, E. M Kober, *Acta Physicochim. URSS* **2009**, *113*, 10619–10640.
[18] Z. Yang, Y. H. He, *Acta Physicochim. URSS* **2016**, *32*, 921–928.
[19] N. Rom, B. Hirshberg, Y. Zeiri, D. Furman, S. V. Zybin, W. A. Goddard, R Kosloff, *J. Phys. Chem. C* **2013**, *117*, 21043–21054.
[20] F. Wang, L. Chen, D. Geng, J. Y. Wu, J. Y. Lu, C Wang, *J. Phys. Chem. A*2018, 122, 3971–3979.
[21] C. X. Ren, X. X. Li, G Li, *Acta Physicochim. URSS* **2018**, *34*, 1151–1162.
[22] R. Z. Miao, W. S. Liu, J. Wang, Z. P. Kang, X. B. Jing, Y. Z. Fu, Y. Q Liu, *Chin. J. Energet. Mater.* **2016**, *24*, 111–117.
[23] D. Z. Guo, Q. An, S. V. Zybin, W. A. Goddard, F. L. Huang, B Tang, *J. Mater. Chem. A* **2015**, *3*, 5409–5419.
[24] L. C. Liu, Y. Liu, S. V. Zybin, H. Sun, W. A Goddard, *J. Phys. Chem. A* **2011**, *115*,11016–11022.
[25] Z. Yang, Y. J. Xue, Y. H. He, *Acta Chim. Sin.* **2016**, *74*, 612–619.
[26] H. Liu, X. Dong, Y. H. He, *Acta Physicochim. URSS* **2014**, *30*, 232–240.
[27] F. Wang, L. Chen, D. Geng, J. Y. Lu, J. Y Wu, *Phys. Chem. Chem. Phys.* **2018**, *20*, 22600–22609.
[28] M. R. Manaa, E. J. Reed, L. E. Fried, N Goldman, *J. Am. Chem. Soc.* **2009**, *131*,5483–5487.
[29] M. S. Shaw, J. D. Johnson, *J. Appl. Phys.* **1987**, *62*, 2080–2085.
[30] H. Liu, Y. H. He, *Acta Armamentarii* **2016**, *37*, 414–423.

Manuscript received: January 13, 2020
Revised manuscript received: March 15, 2020